The published version of the paper "Morbidelli R., Saltalippi C., Flammini A., Corradini C., Brocca L., Govindaraju R.S. (2016). An investigation of the effects of spatial heterogeneity of initial soil moisture content on surface runoff simulation at a small watershed scale. Journal of Hydrology, 539, 589-598." is available at: https://doi.org/10.1016/j.jhydrol.2016.05.067

An investigation of the effects of spatial heterogeneity of initial soil moisture content on surface runoff simulation at a small watershed scale

Renato Morbidelli[1], Carla Saltalippi and Alessia Flammini, Corrado Corradini

Dept. of Civil and Environmental Engineering, University of Perugia, via G. Duranti 93, 06125 Perugia, Italy

Luca Brocca

Research Institute for Geo-Hydrological Protection, National Research Council, Via Madonna Alta 126, 06128 Perugia, Italy

Rao S. Govindaraju

Lyles School of Civil Engineering, Purdue University, West Lafayette, IN 47907

SUMMARY

In addition to the soil saturated hydraulic conductivity, K_s, the initial soil moisture content, θ_i, is the quantity commonly incorporated in rainfall infiltration models for simulation of surface runoff hydrographs. Previous studies on the effect of the spatial heterogeneity of initial soil water content in the generation of surface runoff were generally not conclusive, and provided no guidance on designing networks for soil moisture measurements. In this study, the role of the spatial variability of θ_i at the small watershed scale is examined through the use of a simulation model and measurements of θ_i. The model combines two existing components of infiltration and surface runoff to model the flow discharge at the watershed outlet. The observed values of soil moisture in three experimental plots are combined to determine seven different distributions of θ_i, each used to compute the hydrographs produced by four different rainfall patterns for two initial conditions classified as “dry” soil and “wet” soil. For rainfalls events typically associated with floods, the spatial variability of θ_i at the watershed scale does not cause significant variations in surface runoff for initially dry or wet soils. Furthermore,

[1] Correspondence to: R.Morbidelli, Department of Civil and Environmental Engineering, University of Perugia, Via Duranti 93, 06125 Perugia, Italy. E-mail: renato.morbidelli@unipg.it

when the main objective is to represent flood events a single ground point measurement of θ_i in each area with the same land use may suffice to obtain adequate outflow hydrographs at the outlet.

Key words: Hydrology, Surface runoff modeling, Soil moisture content, Measurement networks

1. Introduction

Theoretical and experimental investigations of soil moisture content as a function of time have been recently carried out to achieve an acceptable representation of many hydrological processes at different spatial scales (Corradini, 2014; Korres et al., 2015), from the local, or point, (Romano, 2014) to the field (Vereecken et al., 2008; Penna et al., 2009; Zehe et al., 2010; Ojha et al., 2014; Vereecken et al., 2014; Martini et al., 2015) to the basin scale (Fang and Lakshmi, 2014; Schröter et al., 2015). Soil moisture influences, for example, the water vapor supply to the atmosphere through the evaporation and evapotranspiration processes from the earth surface, recharge of aquifers, sub-surface transport of pollutants, timing of irrigation, and rainfall-runoff transformation. This paper is focused on the role of heterogeneity in initial soil moisture in the production of surface runoff. For light to moderate rainfall events, surface runoff is generally affected by a significant loss due to infiltration, which is typically expressed as a function of rainfall rate, r, soil saturated hydraulic conductivity, K_s, and initial soil moisture content, θ_i, prior to a rainfall event. In this context, in the mathematical representation of the rainfall-runoff transformation at the field/watershed scale the infiltration process should be described considering the spatial heterogeneity of r, K_s and θ_i.

Several studies showed that K_s can be represented as a random field characterized by a lognormal probability density function (Warrick and Nielsen, 1980; Sharma et al., 1987), and this variability influences the hydrological response of a slope to a uniform rainfall rate (Binley et al., 1989a-b; Saghafian et al., 1995; Corradini et al., 1998; Corradini et al., 2011). Furthermore, formulations of the areal-average infiltration for K_s as a single spatial variable (Smith and Goodrich, 2000; Govindaraju et al., 2001; Corradini et al., 2002) and for a joint spatial variability of K_s and r (Wood et al., 1986; Castelli, 1996; Govindaraju et al., 2006; Morbidelli et al., 2006) were also proposed. The dominant role of the heterogeneity of K_s in the latter studies was also emphasized for frontal rainfalls with coefficient of variation of r (CVr) considerably less than CV of K_s (CVK_s).

The role of the spatial variability of K_s with respect to infiltration and runoff seems to be well-understood, while that of θ_i needs further investigation though CV of θ_i ($CV\theta_i$) is smaller than CVK_s in most fields. For example, Brocca et al. (2009a, 2010) examined the spatial distribution of θ_i in a few plots under natural conditions and showed that θ_i could be assumed as a random variable characterized by a normal probability density function, limited to positive values, with $CV\theta_i$ approximately equal to 0.1. In addition, it is recognized that the values of CVK_s in natural soils are typically in the range (0.3-1.0) (Nielsen et al., 1973; Sharma et al., 1980; Smettem and Clothier, 1989; Ragab and Cooper, 1993). A numerical analysis of the effects of a joint spatial heterogeneity of K_s and θ_i was made by Hu et al. (2015) who showed that runoff was more strongly influenced by the K_s variability.

Grayson et al. (1995) compared runoff simulations for a micro-watershed (2 m^2) using two spatial distributions of initial soil moisture characterized by the same statistical properties. Very different responses to the same rainfall pattern were obtained for a random or an organized θ_i-field. Merz and Plate (1997) examined the dependency of runoff on the spatial organization of θ_i and soil hydraulic properties and found them important for medium rainfall

events. The effects of the spatial heterogeneity of θ_i on surface runoff generation at the small watershed scale (6.3 Km^2) were also investigated by Bronstert and Bardossy (1999) using different spatial distributions of θ_i obtained through interpolation and stochastic methods. Bronstert and Bardossy (1999) noted that spatial variability of θ_i influenced surface runoff, especially when it was a small fraction of rainfall. On the other hand, experimental investigations using indicative values of initial moisture conditions derived by satellite and/or few ground point measurements were found to be sufficient for use in rainfall-runoff simulation models (Goodrich et al., 1994; Grayson and Western, 1998; Aubert et al., 2003; Brocca et al., 2009b). The role of the spatial variability of θ_i on the estimate of surface runoff at the field scale was also examined by Morbidelli et al. (2012), who found rainfall rate and average initial soil water content to be important factors. For heavy rainfall rates the effects of spatial variability of θ_i on surface runoff could be disregarded, but for rainfall events of low intensity over high average soil moisture contents, the effects could be appreciable, and become marked when the latter reduces to very low values. However, cases with low values of both r and average θ_i produce small amounts of surface water and are generally of minor interest in applied hydrology.

An overall analysis of the aforementioned results suggests that the effects of the spatial variability of θ_i on surface runoff generation are not clearly understood because of the differences in the selected simulation approaches as well as in the spatial scales and rainfall patterns.

The main objectives of this paper are (1) to study the link among the simulation approach, spatial scale and rainfall characteristics, (2) to examine the errors that could be incurred due to scarce sampling of θ_i and how that affects the hydrologic responses of a small watershed to different rainfall patterns. A conceptual/semi-analytical model that combines a point infiltration model for erratic rainfall (Corradini et al., 1997) with a kinematic wave model

based on a similarity profile for flow depth over overland regions and stream reaches (Govindaraju et al., 1999) is used here. These components were tested individually and provided accurate results. Simulations have been carried out starting from the results obtained by Morbidelli et al. (2012) at the field scale using measurements of θ_i performed by Brocca et al. (2010) at the local scale. The hydrological response at the watershed scale has been obtained by schematizing the watershed by a network of planes and channels as in Fig. 1 (Hager, 1984; Melone et al., 1998). Simulations have been mainly performed considering θ_i as a random variable and K_s constant through the watershed, besides for the sake of completeness the role of a joint spatial heterogeneity of θ_i and K_s has been shortly investigated.

2. Modeling approach

Simulation of hydrological response at the watershed outlet requires the representation of infiltration, effective rainfall-surface runoff transformation and water routing through the channel networks.

The basic model is set up schematizing a real watershed by a network of planes and channels (see Fig. 1) with θ_i uniform in each plane, but varying from plane to plane, and K_s and r spatially invariable. The models for point infiltration and surface runoff were described in previous studies, and are summarized below for completeness.

To emphasize the specific role of the spatial variability of θ_i, as a first approximation, the random variability of K_s at the field (plane) scale is disregarded. At this scale, Morbidelli et al. (2012) showed that the surface runoff hydrograph at the outlet can be well-approximated simplifying the field of θ_i through the value observed in a site characterized by temporal stability or using, in cases of practical hydrological interest, a value of θ_i observed at the field

scale. Thus, to investigate the role of the spatial heterogeneity of θ_i on surface runoff production at the small watershed scale, a spatially uniform value of θ_i is assumed in each plane.

2.1 *Point infiltration equations*

Following Corradini et al. (1997), the infiltration process is represented combining the depth-integrated Darcy law and the continuity equation under the assumptions of θ_i invariant with depth, z, and dynamic wetting profile, $\theta(z)$, having the shape of a distorted rectangle characterized by a parameter p and a shape factor β (≤ 1) linked with the water content, θ, at the surface. The resultant ordinary differential equation applicable at each time, t, for any rainfall pattern is:

$$\frac{d\theta_0}{dt} = \frac{(\theta_0 - \theta_i)\beta(\theta_0)}{I'\left[(\theta_0 - \theta_i)\frac{d\beta(\theta_0)}{d\theta_0} + \beta(\theta_0)\right]}\left[q_0 - K_0 - \frac{(\theta_0 - \theta_i)G(\theta_i, \theta_0)\beta(\theta_0)pK_0}{I'}\right] \quad (1)$$

where the subscript 0 stands for quantities at the soil surface, q denotes the downward water flux, I' is the cumulative dynamic infiltration depth and G is the net capillary drive depending on the capillary head, ψ, and hydraulic conductivity, K, as:

$$G(\theta_i, \theta_0) = \frac{1}{K_0}\int_{\psi(\theta_i)}^{\psi(\theta_0)} K(\psi)\, d\psi \quad (2)$$

The functional forms of $K(\psi)$ and $\psi(\theta)$ are:

$$K(\psi) = K_s\left[1 + \left(\frac{\psi - d}{\psi_b}\right)^c\right]^{-(3\lambda+2)/c} \quad (3)$$

$$\psi(\theta) = \psi_b\left[\left(\frac{\theta - \theta_r}{\theta_s - \theta_r}\right)^{-c/\lambda} - 1\right]^{1/c} + d \quad (4)$$

where ψ_b is the air entry head, given for soil texture classes by Rawls et al. (1983); θ_s and θ_r are the volumetric soil water contents at natural saturation and residual, respectively; and c, λ

and d are empirical coefficients. Starting from rainfall with $r>K_s$ over an unsaturated soil surface, when $\theta_0=\theta_s$, because $q_0=r$ and $d\theta_0/dt=0$, Eq. (1) provides time to ponding, t_p, as:

$$\int_0^{t_p} r\,dt = \frac{(\theta_s-\theta_i)G(\theta_i,\theta_s)\beta(\theta_s)pK_s}{r-K_s} \tag{5}$$

For $t>t_p$, Eq. (1) is solved to obtain the infiltration capacity, $f_c=q_0$, until $f_c\leq r$ as:

$$f_c = K_s + \frac{(\theta_s-\theta_i)G(\theta_i,\theta_s)\beta(\theta_s)pK_s}{\int_0^{t_p} r\,dt + \int_{t_p}^{t} f_c\,dt} \tag{6}$$

Eq. (1) is used to estimate the redistribution of the wetted profile. Furthermore, if a new complex storm occurs after redistribution, Eq. (1) is adapted considering the possible development of a compound wetting profile and a procedure of profile consolidation. Using numerical solutions of the Richards equation as a benchmark this component of the simulation model was found to represent the infiltration rate with high accuracy also for complex rainfall patterns.

2.2 *Surface Runoff Equations*

The kinematic wave approximation with flow resistance represented by the Manning law (Singh, 1996) is used to describe mathematically the movement of water over a plane. For a plane with homogeneous characteristics in terms of surface roughness and slope, for one-dimensional flow we have:

$$\frac{\partial h}{\partial t} + \frac{1}{n}S_0^{1/2}\frac{\partial h^{m+1}}{\partial x} = E \tag{7}$$

where h is the flow depth, n is the Manning roughness coefficient, m=2/3, S_0 is the plane slope, x is the spatial coordinate in the downslope direction, E is the effective rainfall rate uniform through the plane and the discharge per unit width is expressed by

$$q = \frac{1}{n}S_0^{1/2}h^{m+1} \tag{8}$$

Following Govindaraju et al. (1999), for a plane of length L the solution of Eq. (7) is prescribed in the form:

$$h(x,t) = h_u(t) + h_l(t)\sin\left(\frac{\pi x}{2L}\right) \tag{9}$$

with $h_u(t)$ expressed by the boundary condition as:

$$h_u(t) = h(0,t) = \left(\frac{q_u(t)n}{S_0^{1/2}}\right)^{1/(m+1)} \tag{10}$$

Substitution of Eq. (9) into Eq. (7), after integration over the plane length, leads to:

$$\frac{dh_l}{dt} + \frac{\pi S_0^{1/2}}{2Ln}\left[(h_u + h_l)^{m+1} - h_u^{m+1}\right] + \frac{\pi}{2}\left(\frac{dh_u}{dt} - E\right) = 0 \tag{11}$$

Equation (11) is integrated numerically starting from the initial condition:

$$h_l(0) = \frac{\pi}{2}\left[\underline{h}(0) - h_u(0)\right] \tag{12}$$

resulting from the integration of Eq. (9) over the plane length at t=0, with $\underline{h}(0)$ spatially averaged initial flow depth. The surface runoff per unit width at the plane outlet is given by:

$$q(L,t) = \frac{1}{n}S_0^{1/2}\left[h_u(t) + h_l(t)\right]^{m+1} \tag{13}$$

2.3 *Streamflow Equations*

The kinematic wave approximation with flow resistance described by the Manning law (Woolhiser et al., 1990) is adopted to represent the water movement. The one-dimensional continuity equation is:

$$\frac{\partial A}{\partial t} + \frac{\partial Q}{\partial x} = q_l \tag{14}$$

where A is the area of flow cross section, q_l is the net lateral inflow reaching the stream per unit length and Q is the discharge expressed by:

$$Q = \frac{1}{n} S_0^{1/2} A R^{m} \tag{15}$$

with R hydraulic radius. The flow depth in the stream, H, is approximated in the form:

$$H(x,t) = H_u(t) + H_1(t)\sin\left(\frac{\pi x}{2L}\right) \tag{16}$$

with $H_u(t)=H(0,t)$ given by the upstream boundary condition and, for rectangular cross-sections of width b, expressed through the corresponding discharge Q(0,t) as:

$$\frac{\frac{1}{n} S_0^{1/2} (b H_u)^{m+1}}{(b + 2H_u)^{m}} = Q(0,t) \tag{17}$$

Expressing A and R in terms of b and H and substituting Eqs. (15) and (16) into Eq. (14), after integration over the stream length, L, the following equation is obtained for $H_1(t)$:

$$\frac{bL\frac{dH_u}{dt} + \frac{2bL}{\pi}\frac{dH_1}{dt} + \frac{S_0^{1/2}}{n}\left[b(H_u + H_1)\right]^{m+1}}{\left[b + 2(H_u + H_1)\right]^{m}} - Q(0,t) - L\underline{q_l}(t) = 0 \tag{18}$$

with $\underline{q_l}(t)$ spatially averaged net lateral inflow per unit length. A numerical solution of Eq. (18) can be obtained starting from the initial condition:

$$H_1(0) = \frac{\pi}{2}\left[\underline{H}(0) - H_u(0)\right] \tag{19}$$

deduced from the integration of Eq. (16) over the stream length at t=0 with $\underline{H}(0)$ spatially averaged initial flow depth. The discharge at the stream outlet is:

$$Q(L,t) = \frac{1}{n} S_0^{1/2} \frac{\left\{b\left[H_u(t) + H_1(t)\right]\right\}^{m+1}}{\left[b + 2H(t)\right]^{m}} \tag{20}$$

3. Study watershed and selected data

The study area is a watershed of ~1.6 km^2 located in the Umbria region, Central Italy. Its configuration is shown in Fig. 2 where the hilly topography, with altitudes in the range 288-612 m a.s.l., in addition to the drainage channel network and the related 17 sub-basins is illustrated. The locations of three experimental plots where measurements of soil moisture content were available are also shown in this figure. The main geometric characteristics of the sub-basins, with average slope up to about 30%, are reported in Table 1. The simplified watershed structure with the planes and channels used for model simulations is illustrated in Fig. 3. The model requires, for each plane, the knowledge of land use consisting of grassland (average slope equal to 4%), olive grove (average slope 18%) and holm-oak (average slope 12%) in this watershed. As the olive grove and holm-oak plots are covered by grass, the Manning roughness coefficient is assumed to be constant through the watershed planes, n=0.5 $sm^{-1/3}$, while n=0.05 $sm^{-1/3}$ for the streams. Soil type can be considered fairly uniform through the watershed, thus a soil representative of a silty loam, frequently found in the Umbria region, was selected. The soil hydraulic quantities, used in Eqs. (3) and (4), are rather similar to those used in previous investigations by Morbidelli et al. (2012) and Morbidelli et al. (2014), specifically: K_s=0.75 mmh^{-1}, θ_s=0.46, θ_r=0.04, ψ_b=-400 mm, with the parameters λ=0.2, c=5 and d=50 mm.

For this investigation, measurements of local soil moisture content in Plots 1-3 have been adopted. These measurements were earlier performed in a large number of sampling dates in the period from April to December 2012 (Zucco et al., 2014) by portable Time Domain Reflectometry (see also Tables 2 and 3). Main statistics of the observed data, synthesized through the spatially averaged point moisture content and the corresponding coefficient of variation, are given in Table 2. Among the 23 sampling dates, two data sets characterized by a considerable difference in the average soil moisture content (April 19, 2012 and June 28, 2012) were selected for our simulations. Table 3 summarizes the spatial distribution of

volumetric soil moisture content, observed by Zucco et al. (2014) for these two dates in each experimental plot where 20 local measurements were performed in Plot 1 and 15 in both Plot 2 and Plot 3. The real spatial distributions of soil moisture content in each plot are considered to represent the initial soil moisture content and used to assign the average value of θ_i in each plane in the simulations of surface runoff under different scenarios. In this context, we note that the number of local measurements in each plot is greater than the number of planes with the same soil use. The aforementioned values of θ_s and θ_r were selected as the maximum and minimum value of θ observed, respectively, in the 23 sampling dates.

Three rainfall patterns observed by a raingauge located inside the study watershed within the period from April 19, 2012 to December 18, 2012 were chosen to represent typical storms, from light to heavy (Fig. 4a-c), producing surface runoff in a range of values from just appreciable to significant. This choice was supported by discharge measurements at the outlet of adjacent basins with similar hydrogeological characteristics. In addition, a hyetograph associated with a return period of 5 years, which is applicable for storm sewer design, was also selected (Fig. 4d).

4. Simulation results and their analysis

Simulations of surface runoff by distributed rainfall-runoff models should be carried out combining the spatial variability of K_s, r and θ_i. However, that would result in a practically intractable number of combinations. While our earlier analysis dealt with θ_i at the field scale (Morbidelli et al., 2012), the current study is mainly focused on θ_i at the small watershed scale under the conditions of K_s and r spatially uniform.

For each hyetograph, simulations were performed using the available observations in a given sampling date on the basis of the following seven different spatial distributions of θ_i:

- θ_i uniform through the watershed and equal to the maximum observed value;
- θ_i uniform through the watershed with value obtained by averaging all measurements available for the plots;
- θ_i uniform through each plane with value deduced by averaging all measurements available for the plot with the same land use;
- θ_i uniform in each plane and assumed equal to the minimum value observed in the plot with the same land use;
- θ_i uniform in each plane and assumed equal to the maximum value observed in the plot with the same land use;
- θ_i uniform in each plane and value randomly taken from the measurements performed in the plot with the same land use. In the study watershed this procedure led to assign a local measurement to a single plane, thus each plane with the same land use was associated with a value of θ_i observed in a different location. Two different spatial distributions of θ_i were realized by this "random" approach.

The rainfall-runoff simulation model requires the solution of algebraic equations together with the numerical solution of three ordinary differential equations (Eq. (1), Eq. (11) and Eq. (18)) which can be integrated with little computational effort.

We denote the soil with the higher water content observed on April 19, 2012 as "wet" soil while that with the lower water content referred to June 28, 2012 as "dry" soil. The results obtained by simulations of surface runoff hydrographs for the rainfall patterns of Fig. 4a-c over the wet and dry soils are compared in Figs. 5-7 and Fig. 8, respectively, for all the selected spatial distributions of θ_i. Figure 5a, which refers to the light storm with rainfall depth of 10.4 mm over the wet soil, shows that the extreme hydrographs are generated by the distributions involving the maximum θ_i through the watershed and the minimum value of θ_i for each land use, which lead to the upper and lower curve, respectively. The corresponding

water volumes are 3,356 m^3 and 782 m^3 with peak discharges of 0.6 m^3s^{-1} and 0.14 m^3s^{-1}. In addition, the hydrograph corresponding to the distribution of θ_i with maximum value for each land use involves values of water volume (1,993 m^3) and peak discharge (0.36 m^3s^{-1}) significantly greater than those of the lower curve. The remaining hydrographs are similar with variations in volume and peak discharge within 10% of each other. Furthermore, for the wet soil the maximum values of soil moisture for each land use determine values of θ_s-θ_i rather different in the three plots (Table 3). For this reason, in order to simulate the hydrograph derived from a single measurement made at a sub-optimal location, the distribution with the maximum observed value of θ_i, assumed uniform through the whole watershed, was considered. The same approach, applied for the minimum observed value of θ_i, resulted in limited variations with respect to the lower hydrograph of Fig. 5a. To link our results to those earlier obtained with a joint spatial variability of θ_i and K_s, we performed some simulations of surface runoff hydrograph coupling the random distributions above described for θ_i with random distributions of K_s obtained from a lognormal probability density function with the average value of 0.75 mmh^{-1} and a value of CVK_s=0.6 included in the range (0.3-1.0) typical of natural conditions. In this context K_s was assumed uniform in each plane, but varying from plane to plane. Figure 5b compares the hydrographs for the watershed average value of θ_i and the random distribution 2, taken from Fig. 5a, with that obtained under the same conditions but combining the last distribution of θ_i with a representative random distribution of K_s. As it can be seen the curve for θ_i randomly variable and K_s uniform is very similar to that derived using the watershed average value of θ_i, while the hydrograph simulated with both θ_i and K_s randomly variable is characterized by a significant increase of discharges. These results indicate that the spatial heterogeneity of K_s is much more important than that of θ_i (see also Hu et al., 2015). A comparison of Fig. 5a with Figs. 6 and 7 indicates that the spread between the extreme hydrographs becomes smaller with increasing total

rainfall depth, with ratios between the maximum and minimum water volume decreasing from 4.3 to 2.5 and 1.3, respectively. Similar behavior is noted in peak discharge values. From the same Figs. 5a, 6 and 7 it may be deduced that assuming θ_i randomly variable with values taken from the performed measurements, the corresponding hydrograph is very similar to that resulting from the hypothesis of θ_i uniform through the watershed and equal to the value obtained averaging all measurements.

Simulations were also performed considering rainfall over the dry soil. For each rainfall pattern the hydrographs associated with the different soil moisture distributions exhibited a similar trend, but the differences in volume and peak discharge between the two extreme curves, as well as between each hydrograph and that referred to the watershed average value of θ_i, were found to be greatly increased. As a representative case, Fig. 8 shows the results obtained for the medium rainfall depth (Fig. 4b) with a ratio between the maximum and minimum value of the water volume increased from 2.5 for the wet soil to 4 for the dry soil. Furthermore, as it can be deduced comparing Figs. 6 and 8, also the ratio between each water volume and that of the watershed average experiences substantial increases with values from 1.5 to 2 for the hydrograph associated with the maximum value of θ_i for each land use.

The results obtained with the same total storm depth (21.2 mm) highlight that the role of the spatial variability of θ_i in a wet soil is considerably less important than in a dry soil. However the latter reduces (approximately by a factor of 10) the surface runoff which becomes insignificant for the development of some events of great practical interest, such as flood events. Thus, the spatial heterogeneity of θ_i in a dry soil is of fundamental importance only in a limited number of studies involving small quantities of surface runoff.

Finally, simulations of surface runoff hydrographs generated by the hyetograph of Fig. 4d (total rainfall depth 40.4 mm) over the dry soil were performed. The hydrographs obtained with different spatial distributions of θ_i exhibit very similar characteristics in Fig. 9 with water

volumes ranging from 22,861 m^3 to 26,580 m^3 and peak runoff between 7.1 m^3s^{-1} and 8.1 m^3s^{-1}. In addition, from the simulations shown in Figs. 6 and 8, more limited variations of the hydrographs can be expected when the same rainfall pattern is applied to the wet soil. The last results suggest that, in the design of structures in hydrological practice, the effect of the spatial heterogeneity of θ_i at the small watershed scale is of minor importance.

For wet soils, the aforementioned results indicate that the spatial variability of θ_i has a significant role for light rainfalls, while it becomes of minor interest for heavy rainfall events, and a single measurement of θ_i randomly performed through the watershed would lead to hydrographs sufficiently accurate at the small watershed outlet. For dry soils, the surface runoff hydrograph experiences relatively more pronounced variations for any storm as a result of the enhanced role of infiltration in the reduction of effective rainfall. That is supported by the volumes of surface and subsurface water computed for each distribution of θ_i in the conditions of dry and wet soil. A representative case is that concerning the distribution with θ_i uniform and equal to the watershed average value. For the dry soil the estimated surface and subsurface volumes referred to the hydrograph of Fig. 8 were 513 m^3s^{-1} and 33,523 m^3s^{-1}, respectively, while for the wet soil the corresponding values associated with the hydrograph of Fig. 6 were 5,407 m^3s^{-1} and 28,630 m^3s^{-1}. These results point out that comparable spatial variabilities of θ_i lead to relatively greater variations of surface runoff in the dry soil because the last quantity is reduced by a factor of 10 with respect to the value computed for the wet soil. The last result has a primary role only when processes linked with a very small generation of surface runoff have to be investigated, and implies the necessity of realizing multiple measurements of θ_i. Finally, for designing purposes the knowledge of θ_i at a single site can be considered useful independently of the condition of dry or wet soil.

5. Conclusions

Initial soil moisture content and soil saturated hydraulic conductivity are the two main quantities included in most infiltration models and strictly linked with the generation of surface runoff. It is widely recognized that both are characterized by a random component which makes modeling very difficult.

The basic role of K_s has been substantially shown in a variety of papers, usually under the condition of spatially uniform θ_i. Here we have primarily shown at the small watershed scale the limited role of heterogeneity of θ_i for K_s considered as a constant. In addition, the discharges obtained by a simplified joint spatial distribution of θ_i and K_s, both considered as random variables, experienced a significant increase due to the dominant role of the spatial heterogeneity of K_s. Thus coupling the variability of the two quantities the role of the heterogeneity of K_s mitigates that of θ_i. Furthermore, our simulation model neglects the run-on process. However, this process would lead (Corradini et al., 1998; Morbidelli et al., 2006) to reduce the effect of the spatial variability of θ_i on surface runoff production through the infiltration of downward overland flow in the areas with smaller values of θ_i. Infiltration through macropores, disregarded in this study, would not change the trend of our results because they reduce the role of matric infiltration and therefore of the spatial variability of soil moisture content.

Our investigation indicates that for rainfall events producing typically flood events, the spatial heterogeneity of θ_i does not affect significantly the nature of the surface runoff hydrograph at the small watershed scale, where a single measurement of θ_i may suffice for rainfall-runoff simulations. Finally, for heavy rainfalls, in agreement with the results by Hu et al. (2015), the effects of the random variability of θ_i at the small watershed scale are found to be very limited.

Acknowledgment

This research was mainly financed by the Italian Ministry of Education, University and Research (PRIN 2010/2011).

References

Aubert, D., Loumagne, C., Oudin, L., 2003. Sequential assimilation of soil moisture and streamflow data in a conceptual rainfall runoff model. J. Hydrol. 280, 145-161.

Binley, A., Elgy, J., Beven, K., 1989a. A physically based model of heterogeneous hillslopes, 1, Runoff production. Water Resour. Res. 25(6), 1219-1226.

Binley, A., Elgy, J., Beven, K., 1989b. A physically based model of heterogeneous hillslopes, 2, Effective hydraulic conductivities. Water Resour. Res. 25(6), 1227-1233.

Brocca, L., Melone, F., Moramarco, T., Morbidelli, R., 2009a. Soil moisture temporal stability over experimental areas in Central Italy. Geoderma 148, 364-374.

Brocca, L., Melone, F., Moramarco, T., Morbidelli, R., 2010. Spatial temporal variability of soil moisture and its estimation across scales. Water Resour. Res. 46, W02516, doi: 10.1029/2009WR008016.

Brocca, L., Melone, F., Moramarco, T., Singh, V.P., 2009b. Assimilation of Observed Soil Moisture Data in Storm Rainfall-Runoff Modeling. J. Hydrol. Eng. 14(2), 153-165.

Bronstert, A., Bardossy, A., 1999. The role of spatial variability of soil moisture for modeling surface runoff generation at the small catchment scale. Hydrol. Earth Syst. Sc. 3, 505-516.

Castelli, F., 1996. A simplified stochastic model for infiltration into a heterogeneous soil forced by random precipitation. Adv. Water Resour. 19(3), 133-144.

Corradini, C., 2014. Soil moisture in the development of hydrological processes and its determination at different spatial scales. J. Hydrol. 516, 1-5.

Corradini, C., Flammini, A., Morbidelli, R., Govindaraju, R.S., 2011. A conceptual model for infiltration in two-layered soils with a more permeable upper layer: From local to field scale. J. Hydrol. 410, 62-72.

Corradini, C., Govindaraju, R.S., Morbidelli, R., 2002. Simplified modelling of areal average infiltration at the hillslope scale. Hydrol. Proc. 16, 1757-1770.

Corradini, C., Melone, F., Smith, R.E., 1997. A unified model for infiltration and redistribution during complex rainfall patterns. J. Hydrol. 192, 104-124.

Corradini, C., Morbidelli, R., Melone, F., 1998. On the interaction between infiltration and Hortonian runoff. J. Hydrol. 204, 52-67.

Fang, B., Lakshmi, V., 2014. Soil moisture at watershed scale: remote sensing techniques. J. Hydrol. 516, 258-272.

Goodrich, D.C., Schmugge, T.J., Jackson, T.J., Unkrich, C.L., Keefer, T.O., Parry, R., Bach, L.B., Amer, S.A., 1994. Runoff simulation sensitivity to remotely sensed initial soil water content, Water Resour. Res. 30(5), 1393-1406.

Govindaraju, R.S., Morbidelli, R., Corradini, C., 1999. Use of similarity profile for computing surface runoff over small watersheds, J. Hydrol. Eng. 4(2), 100-107.

Govindaraju, R.S., Corradini, C., Morbidelli, R., 2006. A semi-analytical model of expected areal-average infiltration under spatial heterogeneity of rainfall and soil saturated hydraulic conductivity. J. Hydrol. 316, 184-194.

Govindaraju, R.S., Morbidelli, R., Corradini, C., 2001. Areal infiltration modeling over soil with spatially-correlated hydraulic conductivities. J. Hydrol. Eng. 6(2), 150-158.

Grayson, R.B., Bloschl, G., Moore, I.D., 1995. Distributed parameter hydrologic modelling using vector elevation data: THALES and TAPES-C, Computer models of watershed hydrology, V.P. Singh (ed.), Water Resources Publications, Highlands Ranch, Colo., 669-696.

Grayson, R.B., Western, A.W., 1998. Towards areal estimation of soil water content from point measurements: time and space stability of mean response. J. Hydrol. 207(1-2), 68-82.

Hager, W.H., 1984. A simplified hydrological rainfall-runoff model, J. Hydrol. 74, 151-170.

Hu, W., She, D., Shao, M., Chun, K.P., Si, B., 2015. Effects of initial soil water content and saturated hydraulic conductivity variability on small watershed runoff simulation using LISEM. Hydrol. Sci. J. 60(6), 1137-1154.

Korres, W., Reichenau, T.G., Fiener, P., Koyama, C.N., Bogena, H.R., Cornelissen, T., Baatz, R., Herbst, M., Diekkrüger, B., Vereecken, H., Schneider, K., 2015. Spatio-temporal soil moisture patterns - A meta-analysis using plot to catchment scale data. J. Hydrol. 520, 326-341.

Martini, E., Wollschläger, U., Kögler, S., Behrens, T., Dietrich, P., Reinstorf, F., Schmidt, K., Weiler, M., Werban, U., Zacharias, S., 2015. Spatial and Temporal Dynamics of Hillslope-Scale Soil Moisture Patterns: Characteristic States and Transition Mechanisms. Vadose Zone J. 14 (4), doi: 10.2136/vzj2014.10.0150.

Melone, F., Corradini, C., Singh, V.P., 1998. Simulation of the direct runoff hydrograph at basin outlet. Hydrol. Proc. 12, 769-779.

Merz, R., Plate, E.J., 1997. An analysis of the effects of spatial variability of soil and soil moisture on runoff. Water Resour. Res. 33(12), 2909-2922.

Morbidelli, R., Corradini, C., Govindaraju, R.S., 2006. A field-scale infiltration model accounting for spatial heterogeneity of rainfall and soil saturated hydraulic conductivity. Hydrol. Proc. 20, 1465-1481.

Morbidelli, R., Corradini, C., Saltalippi, C., Brocca, L., 2012. Initial soil water content as input to field-scale infiltration and surface runoff models. Water Resour. Manag. 26, 1793-1807.

Morbidelli, R., Saltalippi, C., Flammini, A., Rossi, E., Corradini, C., 2014. Soil water content vertical profiles under natural conditions: matching of experiments and simulations by a conceptual model. Hydrol. Proc. 28, 4732-4742, doi: 10.1002/hyp.9973.

Nielsen, D.R., Biggar, J.W., Erh, K.T., 1973. Spatial variability of field measured soil-water properties. Hilgardia 42(7), 215-259.

Ojha, R., Morbidelli, R., Saltalippi, C., Flammini, A., Govindaraju, R.S., 2014. Scaling of surface soil moisture over heterogeneous field subjected to a single rainfall event. J. Hydrol. 516, 21-36.

Penna, D., Borga, M., Norbiato, D., Dalla Fontana, G., 2009. Hillslope scale soil moisture variability in a steep alpine terrain. J. Hydrol. 364, 311-327.

Ragab, R., Cooper, J.D., 1993. Variability of unsaturated zone water transport parameters: implications for hydrological modelling, 1. In situ measurements. J. Hydrol. 148, 109-131.

Rawls, W.J., Brakensiek, D.L., Soni, B., 1983. Agricultural Management effects on soil water processes: Part I. Soil water retention and Green-Ampt parameters. Trans. ASAE 26(6), 1747–1752.

Romano, N., 2014. Soil moisture at local scale: Measurements and simulations. J. Hydrol. 516, 6-20.

Saghafian, B., Julien, P.Y., Ogden, F.L., 1995. Similarity in catchment response, 1, Stationary rainstorms. Water Resour. Res. 31(6), 1533-1541.

Schröter, I., Paasche, H., Dietrich, P., Wollschläger, U., 2015. Estimation of Catchment-Scale Soil Moisture Patterns Based on Terrain Data and Sparse TDR Measurements Using a Fuzzy C-Means Clustering Approach. Vadose Zone J. 14 (11), doi:10.2136/vzj2015.01.0008.

Sharma, M.L., Gander, G.A., Hunt, C.G., 1980. Spatial variability of infiltration in a watershed. J. Hydrol. 45, 101-122.

Sharma, M.L., Barron, R.J.W., Fernie, M.S., 1987. Areal distribution of infiltration parameters and some soil physical properties in lateritic catchments. J. Hydrol. 94, 109-127.

Smettem, K.R.J., Clothier, B.E., 1989. Measuring unsaturated sorptivity and hydraulic conductivity using multiple disc permeameters. J. Soil Sci. 40, 563-568.

Singh, V.P., 1996. Kinematic Wave Modeling in Water Resources: Surface Water Hydrology. John Wiley and Sons, New York.

Smith, R.E., Goodrich, D.C., 2000. A model to simulate rainfall excess patterns on randomly heterogeneous areas. J. Hydrol. Eng. 5(4), 355-362.

Vereecken, H., Huisman, J.A., Bogena, H., Vanderborght, J., Vrugt, J.A., Hopmans, J.W., 2008. On the value of soil moisture measurements in vadose zone hydrology: a review. Water Resour. Res. 44, W00D06.

Vereecken, H., Huisman, J.A., Pachepsky, Y., Montzka, C., van der Kruk, J., Bogena, H., Weihermuller, L., Herbst, M., Martinez, G., Vanderborght, J., 2014. On the spatio-temporal dynamics of soil moisture at the field scale. J. Hydrol., 516, 76-96.

Warrick, A.W., Nielsen, D.R., 1980. Spatial variability of soil physical properties in the field. In: D. Hillel (ed.), Applications of Soil Physics. Academic Press, New York, New York, 319-344.

Wood, E.F., Sivapalan, M., Beven, K., 1986. Scale effects in infiltration and runoff production. Proc. of the Symposium on Conjunctive Water Use, IAHS Publ. N. 156, Budapest.

Woolhiser, D.A., Smith, R.E., Goodrich, D.C., 1990. KINEROS, A Kinematic Runoff Erosion Model, U.S. Dep. of Agric., Agric. Res. Serv., Rep. ARS-77.

Zehe, E., Graeff, T., Morgner, M., Bauer, A., Bronstert, A., 2010. Plot and field scale soil moisture dynamics and subsurface wetness control on runoff generation in a headwater in the Ore Mountains. Hydrol. Earth Syst. Sci. 14, 873-889.

Zucco, G., Brocca, L., Moramarco, T., Morbidelli, R., 2014. Influence of land use on soil moisture spatial-temporal variability and monitoring. J. Hydrol. 516, 193-199, doi: 10.1016/j.jhydrol.2014.01.043.

List of Tables

Figure Captions

Fig. 1. Schematic representation of a small watershed by planes and channels.

Fig. 2. Configuration of the study watershed. The locations of the experimental plots and the stream network are also illustrated.

Fig. 3. Simplified representation of the study watershed by planes and channels. Soil use is also shown. The size of each rectangle is related to the drainage area.

Fig. 4. a), b) and c) Observed rainfall patterns used to represent different meteorological conditions from light to heavy storms. d) Design rainfall event obtained from the intensity-duration curve of the measuring station of Perugia (Central Italy) for a 5-years return period, showing an alternate rainfall patter.

Fig. 5. Surface runoff hydrographs generated by the rainfall event of Fig. 4a over the "wet" soil observed on April 19, 2012: (a) simulations performed for different spatial distributions of initial soil moisture content, θ_i, with uniform saturated hydraulic conductivity, K_s; (b) comparison of hydrographs computed for uniform values of both θ_i and K_s, K_s uniform and θ_i randomly variable, and both θ_i and K_s randomly variable.

Fig. 6. Surface runoff hydrographs simulated for different spatial distributions of soil moisture content representing the "wet" soil observed on April 19, 2012. Rainfall event of Fig. 4b.

Fig. 7. Surface runoff hydrographs simulated for different spatial distributions of soil moisture content representing the "wet" soil observed on April 19, 2012. Rainfall event of Fig. 4c.

Fig. 8. Surface runoff hydrographs simulated for different spatial distributions of soil moisture content representing the "dry" soil observed on June 28, 2012. Rainfall event of Fig. 4b.

Fig. 9. Surface runoff hydrographs simulated for different spatial distributions of soil moisture content representing the "dry" soil observed on June 28, 2012. Rainfall event of Fig. 4d.

Highlights (3 to 5 bullet points (maximum 85 characters including spaces per bullet point)

1. The role of spatial heterogeneity of θi on runoff at basin scale is investigated
2. Simulations are based on the use of observed data of θ and rainfall patterns
3. For considerable rainfalls the spatial heterogeneity of θi is not important

Table 1 - Geometric characteristics of the study watershed sub-basins.

Sub-basin n.	Area (km^2)	Average slope (%)	Channel length (m)
1	0.3920	21.72	1264.0
2	0.0752	29.12	271.4
3	0.0268	21.92	88.3
4	0.0460	25.30	98.3
5	0.0948	21.30	429.7
6	0.0464	13.44	203.1
7	0.1696	11.02	409.7
8	0.1092	27.79	471.4
9	0.0944	28.52	346.6
10	0.0400	8.46	208.3
11	0.0448	21.89	119.0
12	0.0460	18.66	42.4
13	0.1940	28.41	701.4
14	0.0676	6.58	301.4
15	0.0596	16.36	98.3
16	0.0068	2.47	88.3
17	0.0680	3.73	324.3

Table 2 - Main statistics of soil moisture content expressed as a percentage (mean and coefficient of variation, CV) for different sampling dates in three experimental plots (Zucco et al., 2014). The measurements in the highlighted dates have been used for model simulations.

Date	Plot 1		Plot 2		Plot 3	
	Mean	**CV**	**Mean**	**CV**	**Mean**	**CV**
Apr 19, 2012	28.7	0.06	32.4	0.08	28.8	0.08
May 02, 2012	24.7	0.18	24.1	0.24	20.8	0.14
May 09, 2012	27.1	0.09	30.1	0.15	27.9	0.11
May 16, 2012	20.2	0.23	20.6	0.19	18.3	0.15
May 23, 2012	27.4	0.09	35.1	0.09	25.9	0.12
May 30, 2012	21.9	0.16	23.1	0.18	19.5	0.16
Jun 07, 2012	25.0	0.12	25.9	0.17	20.4	0.17
Jun 14, 2012	18.5	0.23	18.1	0.14	12.1	0.27
Jun 21, 2012	12.4	0.26	14.8	0.07	11.8	0.15
Jun 28, 2012	7.2	0.21	8.8	0.30	7.1	0.25
Jul 05, 2012	8.3	0.23	11.1	0.27	7.5	0.12
Jul 12, 2012	6.7	0.29	8.6	0.24	7.7	0.08
Jul 19, 2012	4.9	0.38	5.3	0.31	2.9	0.07
Aug 02, 2012	8.5	0.34	4.3	0.24	7.3	0.30
Aug 30, 2012	5.4	0.35	6.9	0.22	8.1	0.14
Sep 06, 2012	18.2	0.27	17.1	0.20	7.6	0.31
Sep 13, 2012	14.2	0.21	15.1	0.15	7.1	0.26
Sep 20, 2012	17.6	0.29	19.4	0.17	8.1	0.32
Sep 25, 2012	8.4	0.49	6.5	0.59	6.8	0.33
Oct 26, 2012	22.5	0.17	28.1	0.08	12.2	0.38
Nov 09, 2012	22.3	0.10	23.5	0.14	23.2	0.14
Nov 16, 2012	26.0	0.17	28.3	0.04	23.2	0.05
Dec 18, 2012	35.0	0.10	39.4	0.06	28.0	0.11
Average	**17.9**	**0.22**	**19.4**	**0.19**	**14.9**	**0.18**

Table 3 - Spatial variability of soil moisture content expressed as a percentage earlier observed (Zucco et al., 2014) in three experimental plots of the study watershed.

	April 19, 2012			*June 28, 2012*		
	Plot 1	**Plot 2**	**Plot 3**	**Plot 1**	**Plot 2**	**Plot 3**
	26.8	31.3	30.3	6.8	5.4	7.1
	29.1	30.3	31.6	7.0	10.4	9.3
	29.6	32.2	33.7	6.3	6.8	6.1
	26.7	30.7	27.5	4.4	8.7	8.3
	28.3	30.5	27.9	8.6	10.5	10.4
	26.6	28.7	28.0	7.3	13.6	8.5
	25.9	35.2	28.4	6.9	13.2	7.5
	29.9	36.5	30.8	6.7	7.7	8.7
	29.3	34.0	26.6	5.1	11.5	4.7
	29.8	30.6	28.8	10.1	6.3	8.0
	25.8	35.2	25.8	7.2	4.9	6.4
	28.5	33.4	28.6	8.2	8.5	6.3
	28.8	36.0	25.0	9.2	6.6	4.4
	28.4	29.5	30.3	5.3	8.9	5.2
	30.2	32.4	28.8	6.3	9.0	5.2
	30.9			8.8		
	29.4			6.8		
	29.5			6.4		
	31.6			9.5		
	29.0			7.9		
Average	**28.7**	**32.4**	**28.8**	**7.2**	**8.8**	**7.1**
St. Dev.	**1.61**	**2.49**	**2.27**	**1.50**	**2.65**	**1.79**
CV	**0.06**	**0.08**	**0.08**	**0.21**	**0.30**	**0.25**

Figure 1

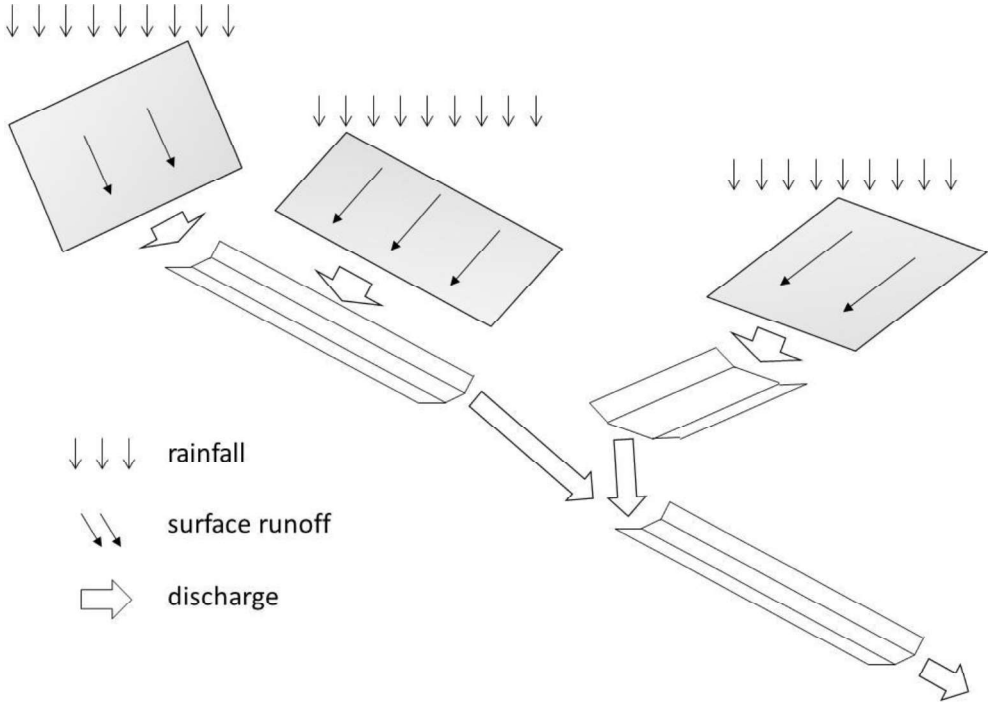

Fig. 1 – Schematic representation of a small watershed by planes and channels.

Figure 2

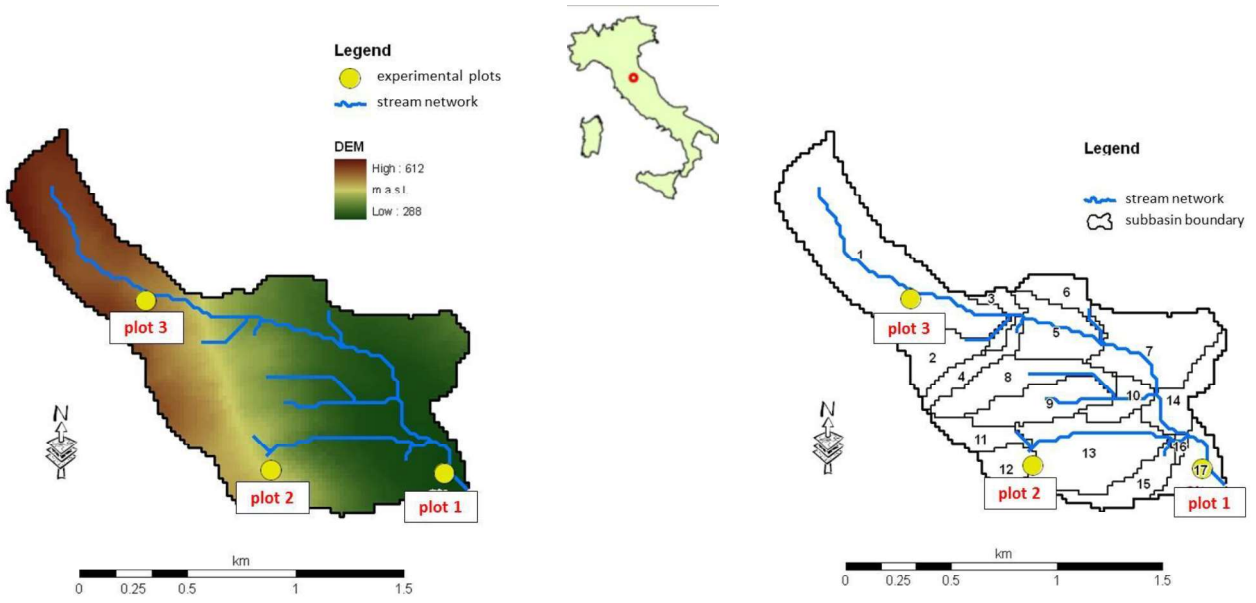

Fig. 2. Configuration of the study watershed. The locations of the experimental plots and the stream network are also illustrated.

Figure 3

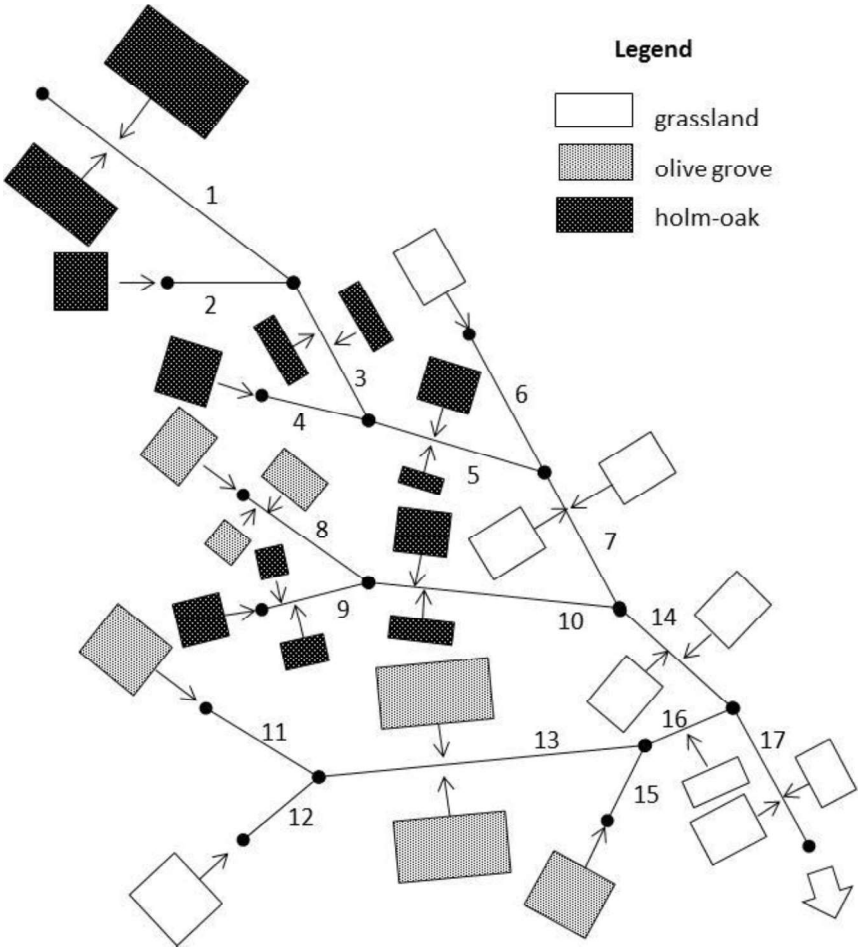

Fig. 3. Simplified representation of the study watershed by planes and channels. Soil use is also shown.

Figure 4

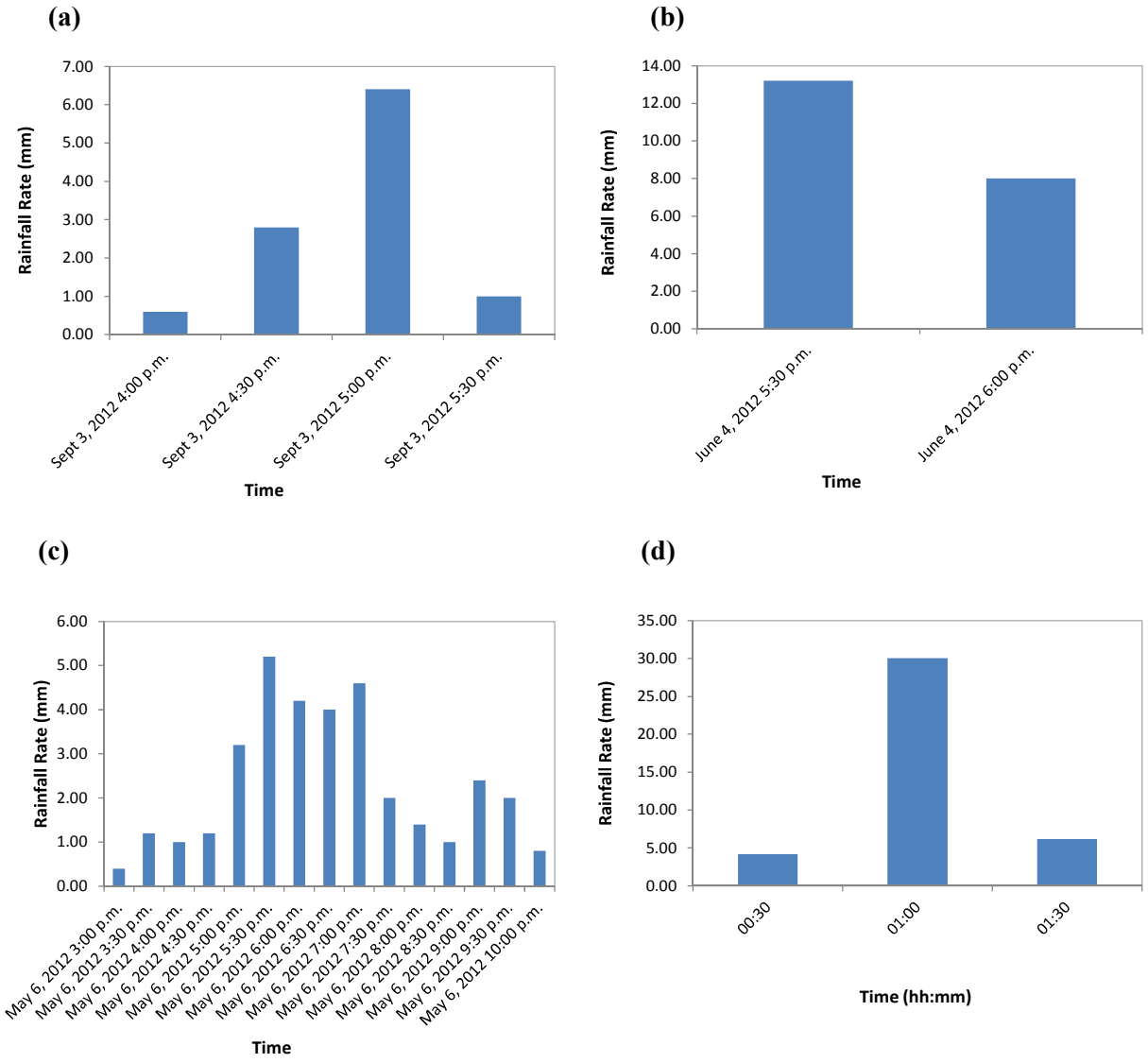

Fig. 4. a), b) and c) Observed rainfall patterns used to represent different meteorological conditions from light to heavy storms. d) Design rainfall event obtained from the intensity-duration curve of the measuring station of Perugia (Central Italy) for a 5-years return period, showing an alternate rainfall pattern.

Figure 5

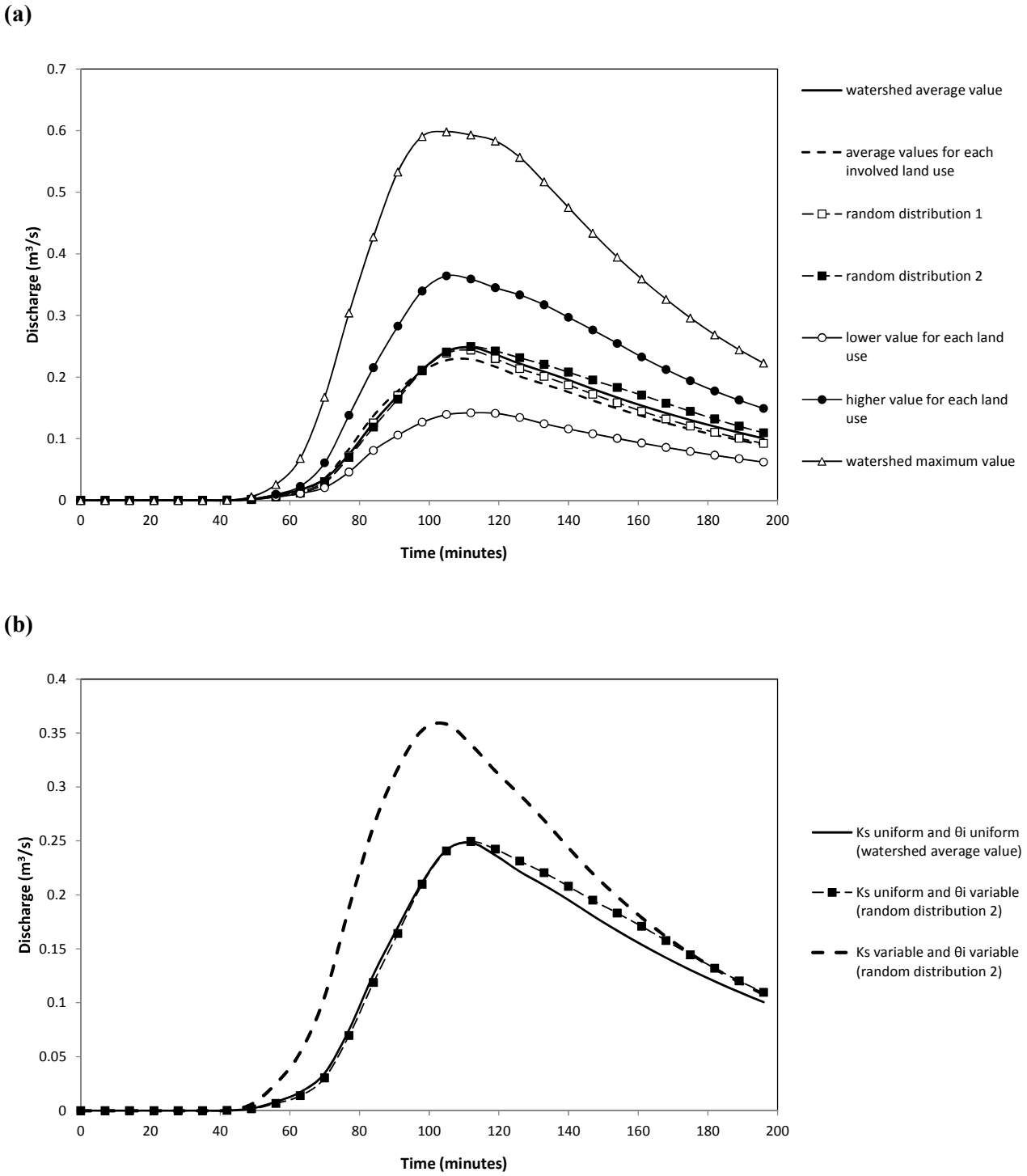

Fig. 5. Surface runoff hydrographs generated by the rainfall event of Fig. 4a over the "wet" soil observed on April 19, 2012: (a) simulations performed for different spatial distributions of initial soil moisture content, θ_i, with uniform saturated hydraulic conductivity, K_s; (b) comparison of hydrographs computed for uniform values of both θ_i and K_s, K_s uniform and θ_i randomly variable, and both θ_i and K_s randomly variable.

Figure 6

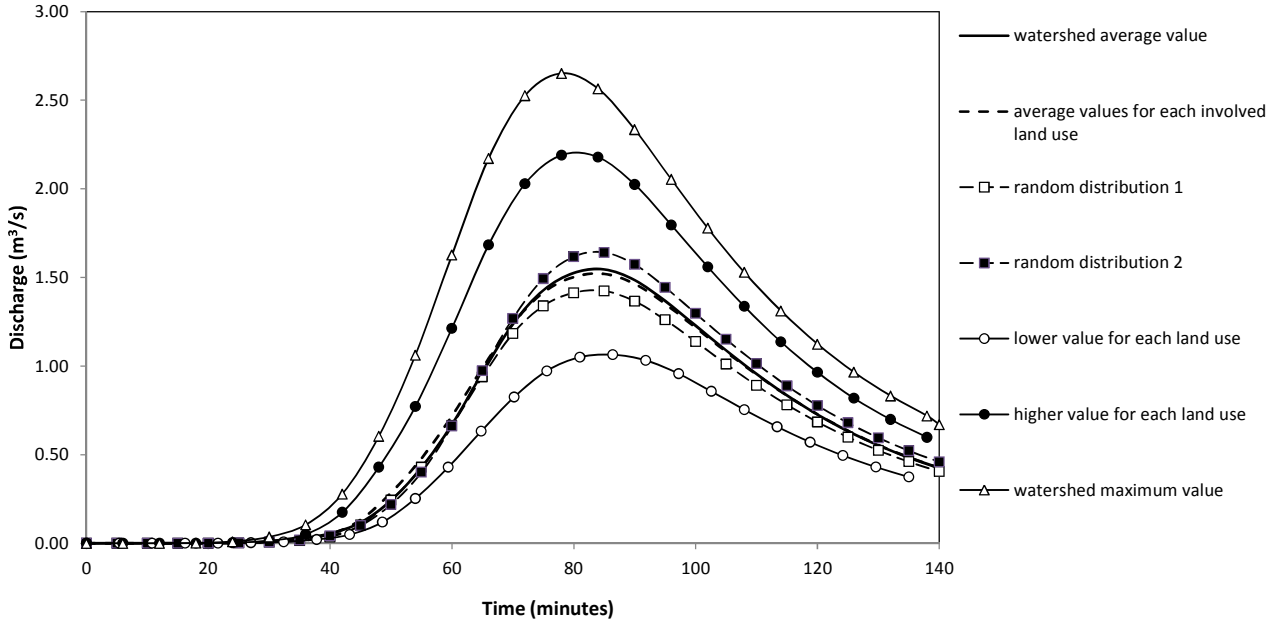

Fig. 6. Surface runoff hydrographs simulated for different spatial distributions of soil moisture content representing the "wet" soil observed on April 19, 2012. Rainfall event of Fig. 4b.

Figure 7

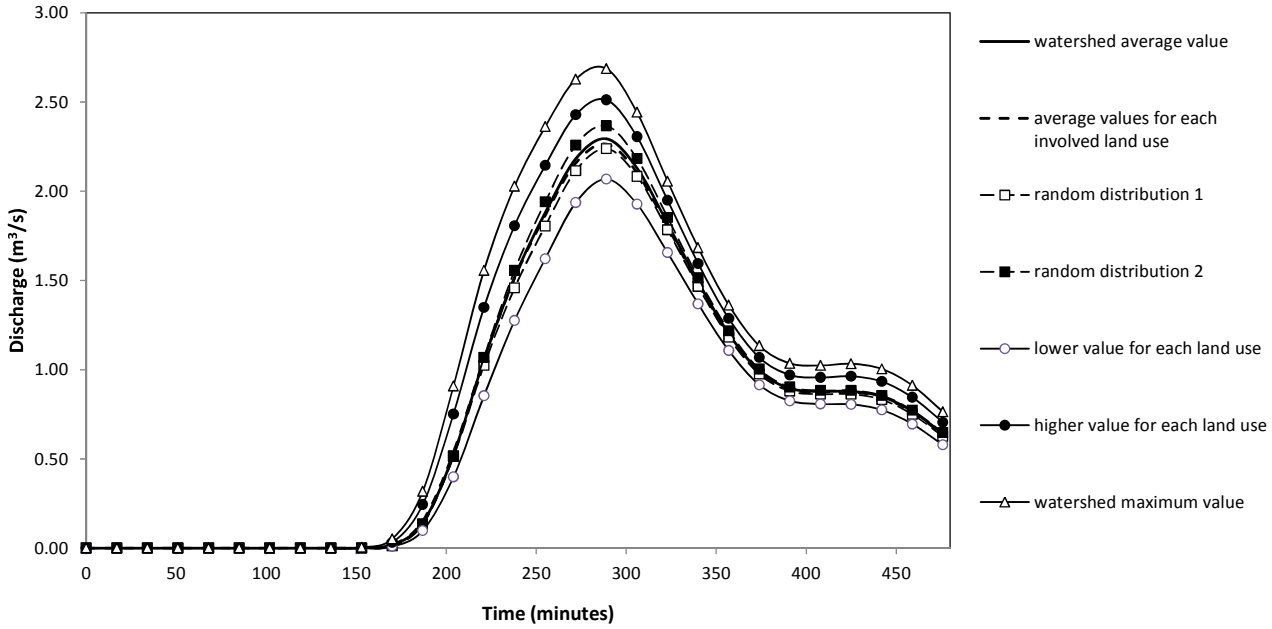

Fig. 7. Surface runoff hydrographs simulated for different spatial distributions of soil moisture content representing the "wet" soil observed on April 19, 2012. Rainfall event of Fig. 4c.

Figure 8

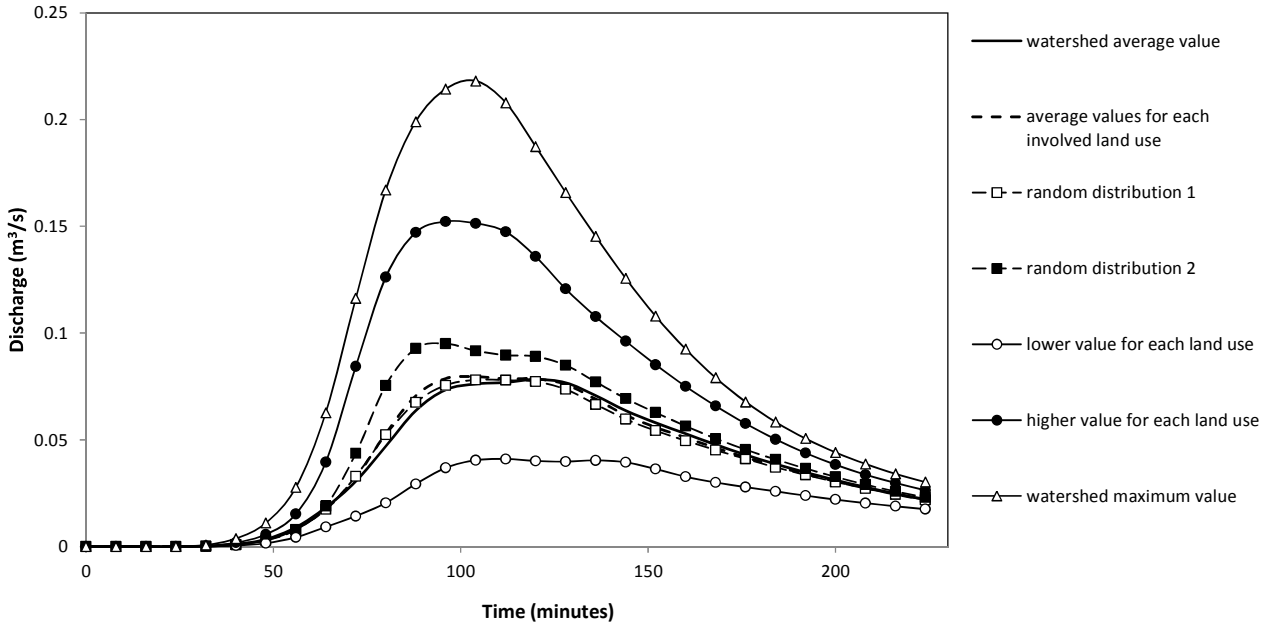

Fig. 8. Surface runoff hydrographs simulated for different spatial distributions of soil moisture content representing the "dry" soil observed on June 28, 2012. Rainfall event of Fig. 4b.

Figure 9

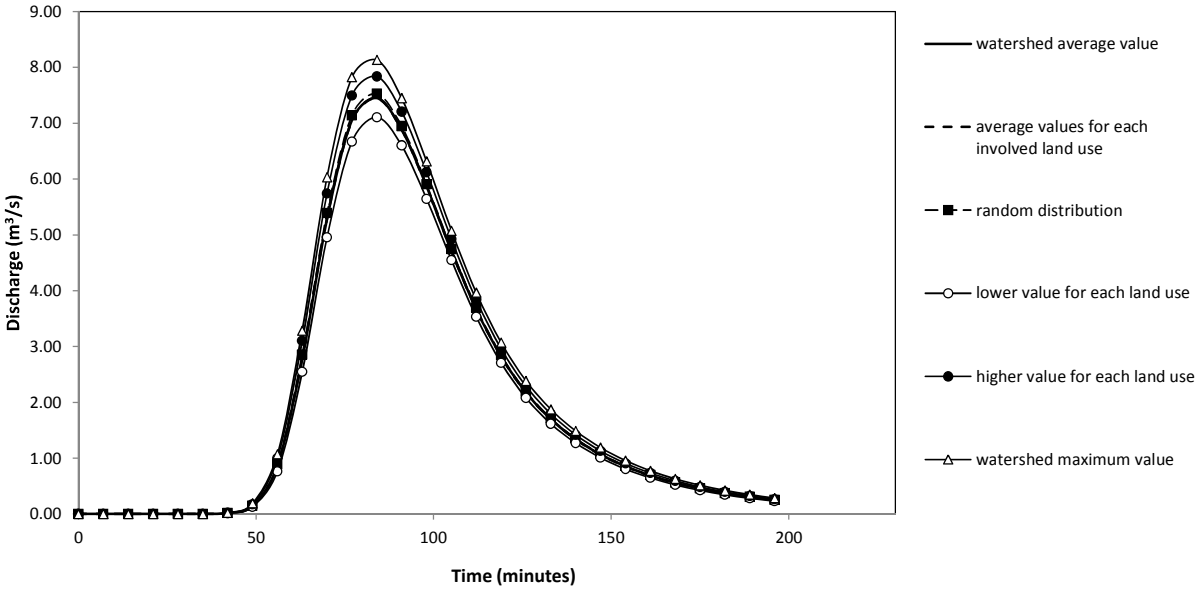

Fig. 9. Surface runoff hydrographs simulated for different spatial distributions of soil moisture content representing the "dry" soil observed on June 28, 2012. Rainfall event of Fig. 4d.